International Review of Automatic Control (I.RE.A.CO.), Vol. 16, N. 3
ISSN 1974-6059 May 2023

Chattering Reduction on Low-Speed Indirect Field Oriented Control Induction Motor Using Second Order Sliding Mode Control

Era Purwanto[1], Abdillah Aziz Muntashir[2], Muhammad Rizani Rusli[1], Bambang Sumantri[1]

Abstract – *Indirect Field Oriented Control is commonly used to control induction motors by allowing separate control of the magnetic flux and torque. However, the changes in motor parameters and load torque to be affecting system stability and performance. To mitigate this issue, a sliding mode control was added to ensure robustness and stability. However, this caused chattering, which can reduce efficiency. A Second-Order Sliding Mode Control was developed to reduce chattering while maintaining system stability and robustness. Lyapunov system stability analysis was also implemented to ensure robustness. The results showed that the Super Twisting Algorithm had a good performance. Meanwhile, Second-Order Sliding Mode Control reduced the chattering up to 2.89 var. This was achieved by maintaining a steady error up to 0.1% at the set point 100 rpm without load. It was also able to retain robustness against changes the changes in load values up to 1.3 N m, even under transient and dynamic conditions.*

Keywords: *Chattering, Indirect Field Oriented Control, Second Order Sliding Mode Control, Super Twisting*

Nomenclature

V_{qs}, V_{ds}	Stator voltage on the d and q axes
V_{dr}, V_{qr}	Rotor voltage on the d and q axes
r_s, r_r	Resistance in the stator and rotor
i_{qr}, i_{dr}	Rotor current on the d and q axes
λ_{dr}, λ_{qr}	Rotor flux on the d and q axes
ω_e, ω_r	Angular speed of rotor and stator
ω_{sl}	Angular speed of speed
L_s, L_r	Inductance of rotor and stator
L_m	Magnetizing inductance
T_e, T_l	Load torque and electric torque
p	Number of poles
J	Moment of inertia
T_r	Rotor time constant
σ	Total leakage factor
s	Sliding surface
α, β	Positive constant
ε, θ, η	Constant
n	Degree of sliding surface
SOSMC	Second Order Sliding Mode Control
IFOC	Indirect Field Oriented Control

I. Introduction

The industrial sector is observed to be consuming approximately 50% of the electrical energy produced in the world [1]. This is associated with the wide application of induction motors because of their large capacity and easy operation. The wide usage of 3-phase induction motors is based on several factors including the simple and strong structure, especially those with cage rotors, relatively low prices, efficiency, and high-power density [2]-[4]. These attributes are based on the absence of brushes with the ability to cause small friction losses as well as high starting torque and reliable torque response under different operating conditions [5]. There is a challenge in the design of a controller for a 3-phase induction motor which is associated with the difficulty in regulating the speed with a coupled system and measuring some electric rotor variables [1]. Therefore, the achievement of an easier analysis and control of a 3-phase induction motor requires first changing the coupled system to a decoupled system also known as vector control. This is necessary to achieve the same behavior as a DC motor [6] where torque and flux can be controlled independently via two stator current input signals. An example of this vector control technique is Field-Oriented Control (FOC) which is further categorized into two based on the method applied to estimate the slip value between the field orientations in the stator and rotor [7]. The Indirect Field-Oriented Control (IFOC) allows easier calculation of slips using the rotor and stator angles with the assistance of the speed sensors, and this is the reason for its wide application in industries [7].

In contrast, the induction motor performance decreased due to the nonlinear dynamic nature of its parameters and changes in load. This led to the implementation of several control methods such as the PID linear controller [8]. It was discovered that the response is quite good in static conditions but slow in dynamic conditions, thereby, indicating the lack of a

 https://doi.org/10.15866/ireaco.v16i3.23474

robust response speed. Therefore, fuzzy logic control was developed but the results were also not good under dynamic load conditions and the system was very dependent on design rules and membership functions.

Variable structure control with the ability to resist nonlinear dynamics uncertainty was adopted using Sliding Mode Control (SMC). This SMC was observed to have several good features such as resistance to parameter variations or load disturbances, fast dynamic response, and simplicity of design and implementation.

Several studies have been conducted in relation to SMC in induction motor settings. For example, those with IFOC were reported to have good performance and resilient to parameter variations and load disturbances [9], [10].

SMC also provided better response and lower overshoot compared to PI controllers and fuzzy PI [11]-[13], [26]. Meanwhile, the first-order sliding mode control was observed to have certain drawbacks such as the maintenance of the status trajectory on the sliding surface which caused oscillations or chattering [14]. It also leads to the stability of the control system and high-power loss [15] which is dangerous to the implementation process. Moreover, the high-frequency chattering phenomenon was linked to the variable control input due to the discontinue function [16]. Efforts have been made to reduce this phenomenon as indicated by the application of Boundary-SMC at low-speed settings of induction motors but the stability was observed to have been reduced. This caused an increase in the steady error under dynamic conditions [4]. Induction motors are usually difficult to control at low-speed settings. This is due to the loss of excessive power which subsequently has a great effect on the low-speed response of the motor, thereby, leading to a greater percentage of chattering.

Therefore, this study used the second-order sliding mode control to reduce the chattering phenomenon without ignoring the robustness. Super twisting was also applied to produce a good and convergent tracking trajectory within a limited time [17]. Moreover, Lyapunov stability analysis was used to guarantee system stability. The application of the second-order sliding mode control was expected to improve dynamic performance, minimize power losses caused by chattering, and increase induction motor efficiency. This proposed control strategy was observed through simulations and experiments using Labview.

This paper is structured as follows. In the following section, the mathematical dynamic model of indirect field oriented control is derived in Section II. The proposed methodology is that the second order Sliding Mode Control design is presented in Section III, by analyzing the stability of the system using the Lyapunov stability presented in Section IV. Then the results and analysis obtained by simulation and hardware testing are presented in Sections V and VI. Finally, the concluding remarks are given in Section IV. The future work can be developed by increasing the decoupling current control, so it can be increased efficiency system, and can be developed by replacing the algorithm used, to improve response performances.

II. Modelling the Indirect Field Oriented Control (IFOC)

A 3-phase induction motor is ideally assumed to be symmetrical. This is the reason the reference frame dq0 is usually set based on the position that matches the components of the motor analysis used. This study used a stationary reference frame as a dq0 for the dynamic model of an induction motor as shown in Figures 1 [18], [27]. The ABC coordinate system was also transformed to dq coordinate system using Equation (1), where the variable *f* could be in the form of voltage, current, or flux as follows [19]:

$$fqds = T(\theta)\, fabcs \tag{1}$$

The induction motor modeling equation is presented in the following Equations (2)-(5) [19]:

$$\frac{di_{qs}}{dt} = \frac{1}{\sigma L_s}\left[-R_{sm} i_{qs} + \omega_s \sigma L_s i_{ds} + + \frac{L_m}{L_r}\left(\frac{\lambda_{qr}}{T_r} + P\omega_r \lambda_{dr}\right) + V_{qs}\right] \tag{2}$$

$$\frac{di_{sd}}{dt} = \frac{1}{\sigma L_s}\left[-R_{sm} i_{sd} + \omega_s \sigma L_s i_{sq} + + \frac{L_m}{L_r}\left(\frac{\lambda_{rd}}{T_r} + P\omega_r \lambda_{rq}\right) + V_{sd}\right] \tag{3}$$

$$\frac{d\lambda_{qr}}{dt} = \frac{L_m}{T_r} i_{qs} + \omega_{sl} \lambda_{dr} - \frac{1}{T_r}\lambda_{qr} \tag{4}$$

$$\frac{d\lambda_{dr}}{dt} = \frac{L_m}{T_r} i_{ds} + \omega_{sl} \lambda_{qr} - \frac{1}{T_r}\lambda_{dr} \tag{5}$$

The IFOC was used to adjust the field in an induction motor to change the coupled system was changed to a decoupled system. The process involved aligning the flux component (λ_r) at the current I_d with the d-axis and the torque component T_e at the current I_q with the q axis.

This system allowed the separate adjustment of flux and torque current. The IFOC equation obtained is presented in the following (6)-(8):

$$\frac{di_{sd}}{dt} = \frac{1}{\sigma L_s}\left[-R_{sm} i_{sd} + \omega_e \sigma L_s i_{sq} + \frac{L_m}{L_r}\left(\frac{\lambda_r}{T_r}\right) + V_{sd}\right] \tag{6}$$

$$\frac{di_{sq}}{dt} = \frac{1}{\sigma L_s} \times \times \left[-R_{sm} i_{sq} + \omega_e \sigma L_s i_{sd} + \frac{L_m}{L_r}(P\omega_r \lambda_r) + V_{sq}\right] \tag{7}$$

$$\frac{d\lambda_r}{dt} = \frac{L_m}{T_r} i_{sd} - \frac{1}{T_r}\lambda_r \tag{8}$$

The equation for the rotational speed of the rotor and torque is stated in (9) and (10) [4]:

$$\omega_r = \int (T_e - T_l)\frac{p}{2J} \tag{9}$$

$$T_e = \frac{3}{2}\frac{P}{2}\frac{L_m}{L_r}(\lambda_r i_{qs}) \tag{10}$$

The substitution of the flux equation into the rotor voltage equation produced the approximate value of the flux as shown in Equation (11) [4]:

$$\lambda_r = \frac{L_m i_{ds}}{T_r s + 1} \tag{11}$$

with $\tau_r = \frac{L_r}{R_r}$. The determination of the angle theta (θ_e) required obtaining the IFOC value from the speed sensor while the flux angle for the transformation was determined using the rotating speed (ω_r) and the slip speed (ω_{sl}) as indicated in Equations (12) and (13) [6]:

$$\theta_e = \int \omega_e dt = \int (\omega_r + \omega_{sl})dt \tag{12}$$

$$\omega_{sl} = \frac{L_m R_r}{\lambda_r L_r} i_{qs} \tag{13}$$

III. Design of Second Order Sliding Mode Control (SOSMC)

The chattering phenomenon was reduced while the robust system was also maintained at the same time using the High-Order Sliding Mode Control (SOSMC) applied in this study [24], [25]. This was based on the principle that the discontinue function was shifted from the first order to the second or higher order. The algorithm used was the super twisting which has the ability to retain the main advantages of the first-order shear mode, the robustness, and converge to the origin asymptotically or within a limited time [17] in addition to the reduction of chattering [20]. Moreover, control error and its integral were applied to the algorithm on a control surface. This method combined the main advantages of sliding mode and conventional linear controls [12], [23]. Therefore, the general equation of the super-twisting control system is shown in (14)-(16) [21]:

$$u(t) = u_1(t) + u_2(t) \tag{14}$$

with:

$$u_1(t) = -\alpha\sqrt{|x(t)|}sign[x(t)], \alpha > 0 \tag{15}$$

$$\dot{u}_2(t) = -\beta sign[x(t)], \beta > 0 \tag{16}$$

The design of the SOSMC required the mathematical modeling of the system to be controlled which, in this case, was the rotor speed of an induction motor.

Therefore, the speed controller of the IFOC was modeled mathematically as previously discussed. In designing the control, the input u on SOSMC was observed not to be much different from FOSMC with the only variation associated with the u_{smc} control signal value.

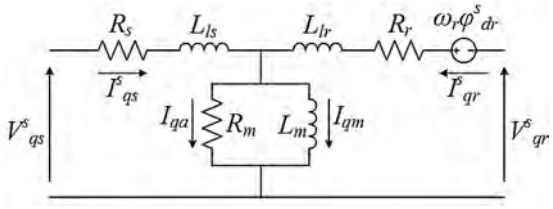

Figs. 1. dq axis equivalent circuit: (a) q-axis (b) d-axis

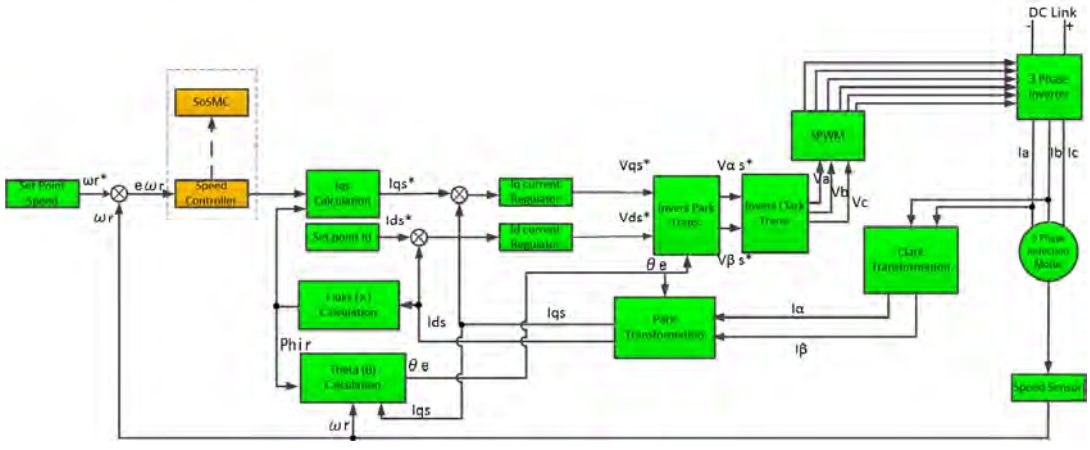

Fig. 2. SOSMC scheme on IFOC

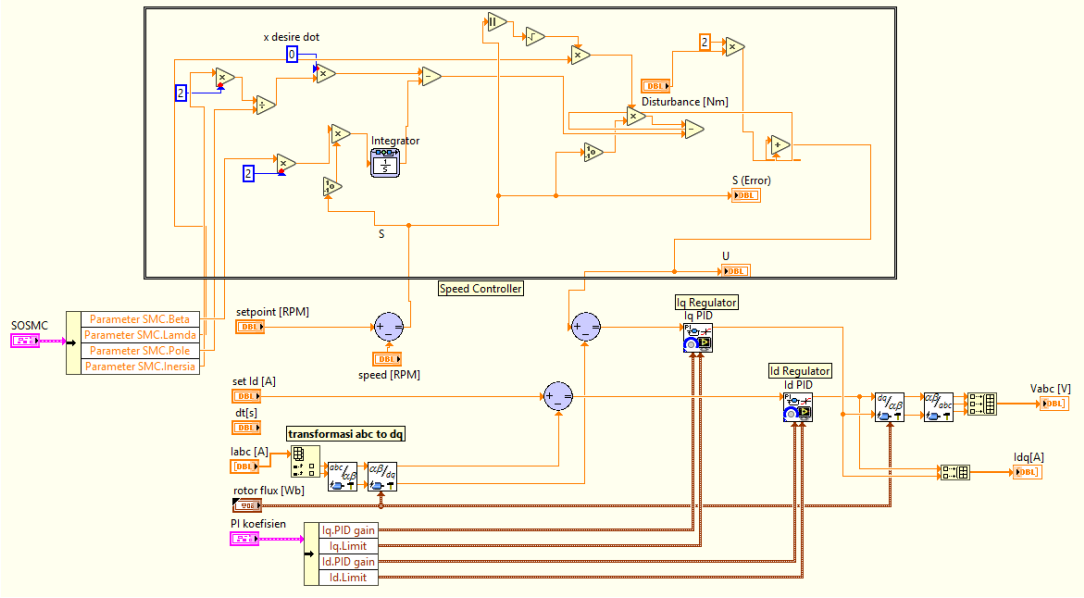

Fig. 3. SOSMC program on IFOC

Therefore, the control input u was obtained using Equation (17):

$$u = u_{eq} + u_{smc} \tag{17}$$

with $u_{eq} = \frac{2J}{P}\left(\dot{\omega}_{r(desire)}\right)$, $u_{smc} = u_{ST} = u_1 + u_2$, here u_1 and u_2 are presented in Equations (15) and (16). This led to the reformulation of the control SOSMC Super Twisting as in Equation (18):

$$u = \frac{2J}{P}\left(\dot{\omega}_{r(desire)}\right) + \\ -\left(\alpha|s|^{0.5} sign(s)\right) - \int\left(\beta sign(s)\right) \tag{18}$$

The values of the parameters α and β were subsequently determined through the Lyapunov stability analysis theorem.

IV. Lyapunov Stability

The stability of the control design was analyzed using the Lyapunov stability method [26], [28].

The application of this technique to a second-order system required formulating a new equation as presented in (19) and (20) [22]:

$$\dot{s} = -\varepsilon|\sigma_\omega|^{\frac{1}{2}} sign(s) + \theta\varphi_\omega \tag{19}$$

$$\dot{\varphi}_\omega = -\eta\, sign(s) \tag{20}$$

with $\varepsilon, \theta, \eta$ = constant. The system was stable or converged to 0 when the following two conditions were fulfilled [16]:

- $V(s,\varphi) = \zeta^T P \zeta$ → positive definite (v>0);
- $\dot{V}(s,\varphi) = \zeta^T P \dot{\zeta} + \dot{\zeta}^T P \zeta$→ negative definite ($v$<0).

This means $V(s,\varphi) = \zeta^T P \zeta$ → positive definite (v>0), with:

$$\zeta^T = \begin{bmatrix} |s|^{\frac{1}{2}}, \varphi_\omega \end{bmatrix}$$

$$P = \frac{1}{2}\begin{bmatrix} 4\eta + \varepsilon^2 & -\varepsilon\theta \\ -\varepsilon\theta & 2\theta^2 \end{bmatrix}$$

P = positive symmetric matrix

The matrix P was also expected to have a positive symmetry for condition V to produce a positive definite.

The parameter values ε,θ,η used also needed to fulfill the requirements of the positively symmetrical P matrix:

$$\dot{V}(s,\varphi) = \zeta^T P \dot{\zeta} + \dot{\zeta}^T P \zeta \rightarrow \textit{negative definite}\ (v<0)$$

where:

$$\dot{\zeta} = \begin{bmatrix} \dot{s} \\ 2|s|^{\frac{1}{2}} \\ \dot{\varphi}_\omega \end{bmatrix} = -\frac{1}{|s|^{\frac{1}{2}}}\begin{bmatrix} \frac{\varepsilon}{2}|s|^{\frac{1}{2}} sign(s) - \frac{\theta}{2}\varphi_\omega \\ \eta|s|^{\frac{1}{2}} sign(s) \end{bmatrix} = \\ = -\frac{1}{|s|^{\frac{1}{2}}}\begin{bmatrix} \frac{\varepsilon}{2} & -\frac{\theta}{2} \\ \eta & 0 \end{bmatrix}\zeta$$

This means:

$$\dot{V}(s,\varphi) = \zeta^T P \dot{\zeta} + \dot{\zeta}^T P \zeta = \\ = -\frac{1}{|s|^{\frac{1}{2}}}\zeta^T\left(P\begin{bmatrix} \frac{\varepsilon}{2} & -\frac{\theta}{2} \\ \eta & 0 \end{bmatrix} + \begin{bmatrix} \frac{\varepsilon}{2} & \eta \\ -\frac{\theta}{2} & 0 \end{bmatrix}^T P\right)\zeta = \\ = -\frac{1}{|s|^{\frac{1}{2}}}\zeta^T X \zeta$$

where:

$$X = \frac{1}{2}\begin{bmatrix} 4\varepsilon\eta + \varepsilon^3 - 2\varepsilon\theta\eta & -2\theta\eta\varepsilon^2\theta + 2\theta^2\eta \\ -2\theta\eta - \varepsilon^2\theta + 2\theta^2\eta & \varepsilon\theta^2 \end{bmatrix}$$

X = positive definite

The positive symmetry P matrix value provided a definite positive value for the X matrix. Therefore, the second condition which was $V(s,\varphi)$ needed to be negative definite and this was fulfilled.

V. Simulation Results

The simulation was conducted using the Labview software to determine and observe the performance of the controller designed. The chain block from the SOMC simulation is shown in the Figure 3. The parameter values of the 3-phase induction motor used are also listed in Table I. The speed response results presented in Figures 4 and 5 show that the SOSMC had good dynamic performance and the ability to reduce the percentage of chattering phenomena. The graph also indicated that the robustness was maintained at the set point value when there was a disturbance (load torque).

TABLE I
3-PHASE INDUCTION MOTOR PARAMETERS

Parameter	Value	Unit
R_{stator}	5,26	Ω
R_{rotor}	6,47	Ω
L_{stator}	44,7	m H
L_{rotor}	26,9	m H
$L_{magnetization}$	128	m H
inertia	0,13	kg m^2
pole	4	

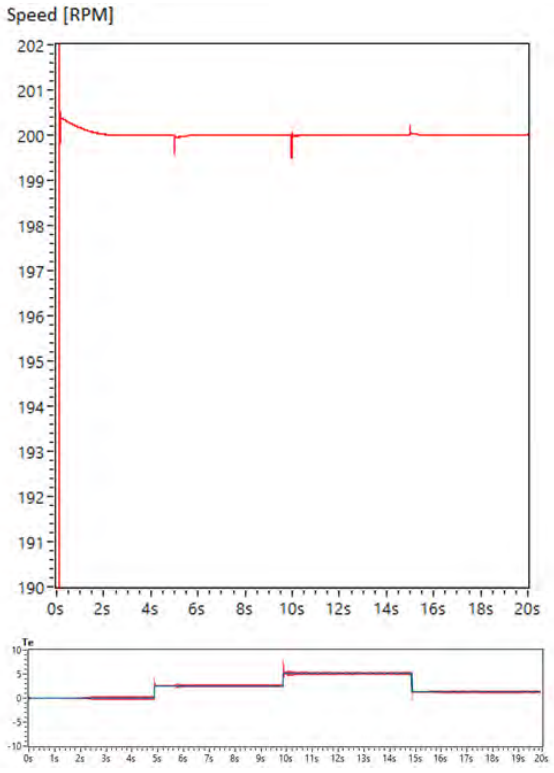

Fig. 4. SOSMC simulation at a set point of 200 Rpm

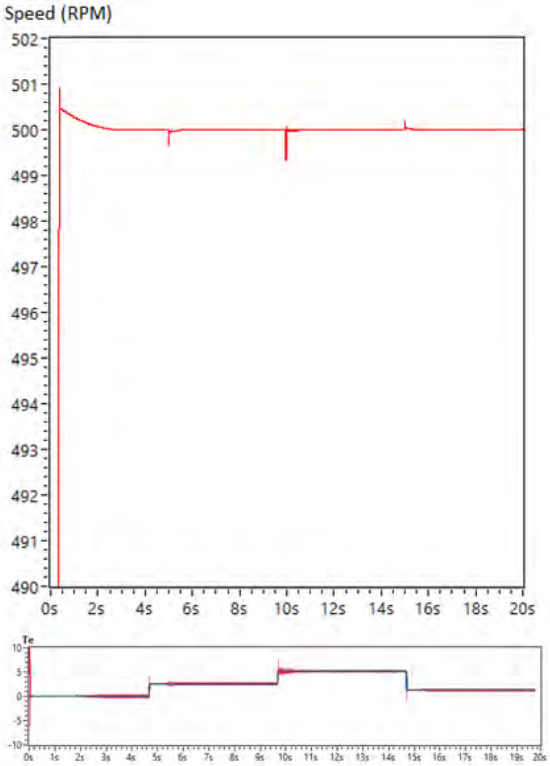

Fig. 5. SOSMC simulation at a set point of 500 Rpm

This was due to the advantages of SOSMC associated with the reduction of chattering phenomena percentage using the continue function. Moreover, the super twisting algorithm used an integral function to ensure robustness against disturbance. The results of the controller performance from the response are presented in the following Table II.

The results presented in Table II show that the use of SOSMC to control the speed of a 3-phase induction motor based on IFOC was able to reduce the chattering phenomenon to 0.001 var.

It also had the ability to provide a very fast transient response towards a steady state when viewed from the response time perspective. Moreover, SOSMC kept the system robust when there was a disturbance (load torque), thereby, leading to the production of a small steady error. It also had an overshoot value of up to 3% at a set point of 100 rpm.

VI. Experimental Results

The hardware used in this study consists of several parts including a 3-phase inverter as 1, its driver as 2, myrio as 3, the connector/input to the motor as 4, and the current sensor as part 5 as indicated in Figure 6. The mechanical design of the 3-phase induction motor had a couple in the form of the DC motor applied as the load.

An IFOC test was conducted using the First Order Sliding Mode Control (FOSMC) without a load on the speed setting of the 3-phase induction motor and the set point value was varied.

TABLE II
SOSMC SIMULATION PERFORMANCE
WITH SOMC PARAMETER α=30 AND β=4

Setpoint	Dead Time (ms)	Rise Time (s)	Settling Time (s)	Error Steady State (%)	Chattering (Var)	Overshoot (%)
100	23,52	0,04791	0,052	0,001	0,046	3
200	31,38	0,08806	0,056	0,0017	0,028	1,5
300	37,87	0,1358	0,145	0,0014	0,0057	0,5
400	43,68	0,19334	0,22	0,0017	0,0031	0,275
500	49,32	0,26293	0,3	0,001	0,0022	0,18

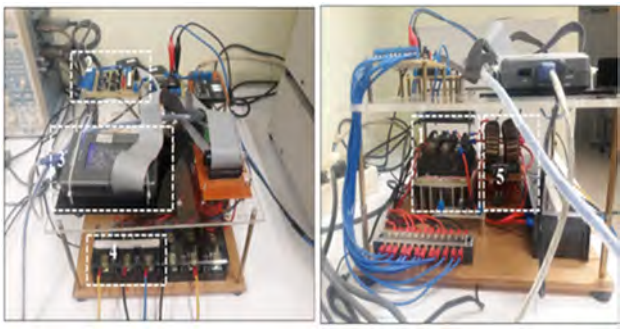

Fig. 6. Experimental Setup

The motor was set at a low speed with a set point value ranging from 100 rpm to 500 rpm, and the FOSMC parameter values used were $\alpha = 100$ and $k = 15$. The motor speed response obtained at 500 rpm without a load is presented in Figure 7. It shows that the system rotor speed was robust and stable at the set point value. It was also observed that the FOSMC had a fast transient response but there was a chattering phenomenon in the velocity response graph as indicated by the change in oscillating value with high frequency on the sliding surface. This was a weakness of the Sliding Mode Control (SMC). Moreover, the chattering phenomenon was caused by the sign(s) function associated with the discontinuity in the control signal designed, thereby, leading to a change in the control input u value. Another IFOC test was conducted using SOSMC without load and the set point value was also varied. The motor was set at low speed with a set point value ranging from 100 rpm to 500 rpm. The SOSMC parameter values used include $\alpha = 3$ and $\beta = 10$ obtained through Lyapunov stability analysis. The motor speed response obtained at 100 rpm until 500 rpm without load is shown in Figures 8-12.

TABLE III
SOSMC AND FOSMC PERFORMANCE WITHOUT LOAD

Setpoint	Chattering (Var)		Rise Time (s)		Settling Time (s)		Error Steady State (%)	
	SOSMC	FOSMC	SOSMC	FOSMC	SOSMC	FOSMC	SOSMC	FOSMC
100	2,89	25	0,22	0,27	1,08	0,51	0,1	0,25
200	1,21	21,26	0,45	0,48	1,1	0,79	0,1	0,22
300	0,64	20,25	0,67	0,65	1,35	0,88	0,12	0,21
400	0,36	19,36	0,88	0,89	1,56	1,08	0,12	0,21
500	0,16	16	1,1	1,01	0,3	1,19	0,12	0,21

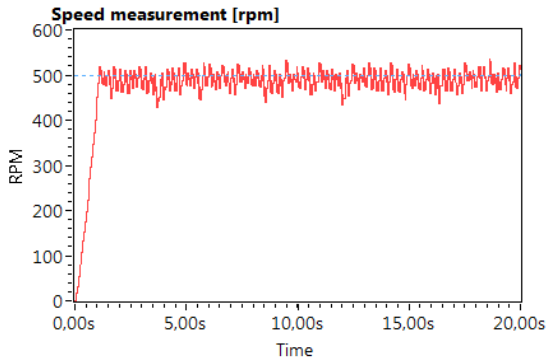

Fig. 7. FOSMC without load at 500 rpm set point

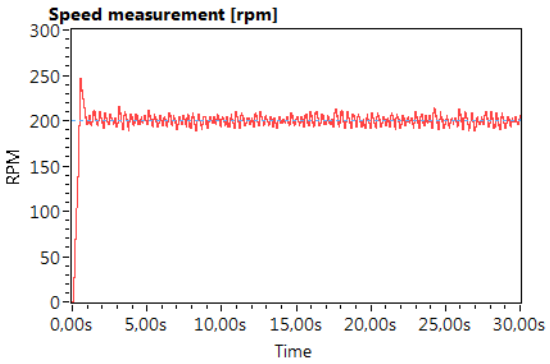

Fig. 9. SOSMC without load at 200 rpm set point

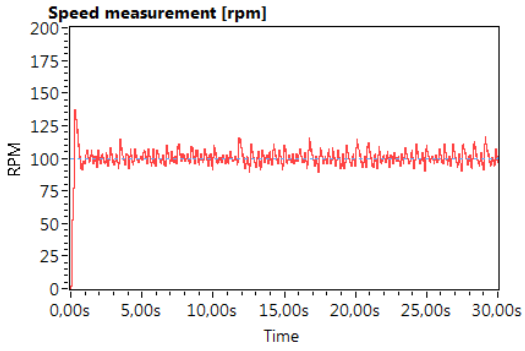

Fig. 8. SOSMC without load at 100 rpm set point

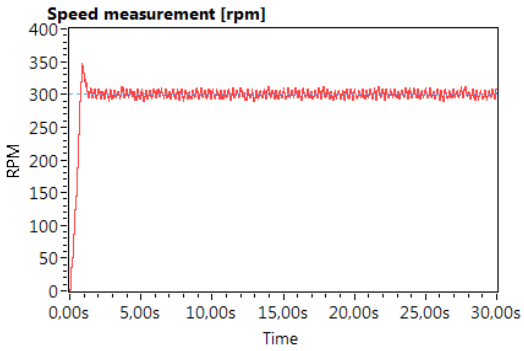

Fig. 10. SOSMC without load at 300 rpm set point

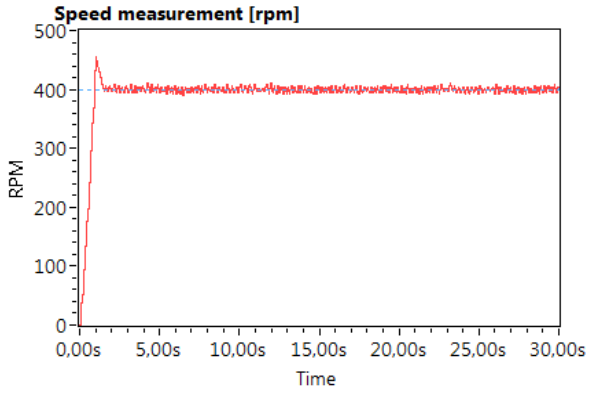

Fig. 11. SOSMC without load at 400 rpm set point

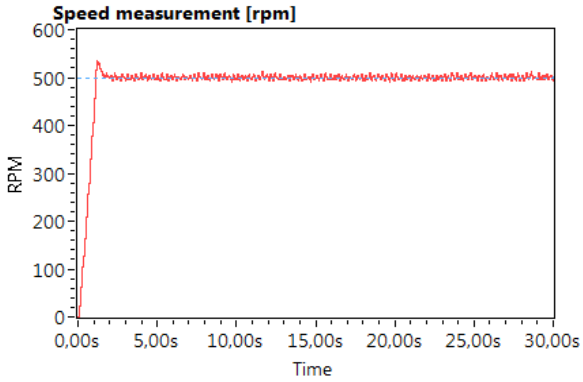

Fig. 12. SOSMC without load at 500 rpm set point

The results showed that the application of SOSMC without load was able to reduce the percentage of the chattering phenomenon. This was due to the application of the continue function in the super-twisting algorithm which was an advantage of the control model. It was also observed that the speed response had a pretty good transient response with a small and steady error value.

Table III compares SOSMC with FOSMC in the speed regulation of 3-phase induction motors based on IFOC no-load conditions. It was discovered that the SOSMC had the least percentage of chattering phenomena by reducing the value up to 2.9 var at the 100 rpm set point.

Meanwhile, there was no difference between the two mode controls for the transient response. It was observed that FOSMC had a faster response at settling time and this was because SOSMC had an overshoot which increased the time to achieve a steady state. The two modes were also found to have the ability to produce small steady errors but SOSMC had a slightly smaller value. The determination of the robustness of the SOSMC super twisting control system designed for the speed regulation of the 3-phase induction motor required testing the system under dynamic conditions. The 3-phase induction motor was loaded with a coupled DC motor from an external source. Moreover, the supply of a large input voltage to the DC motor ensured its rotation in the opposite direction of the 3-phase induction motor to load. The setup for the SOSMC test circuit with a load is shown in Figure 13.

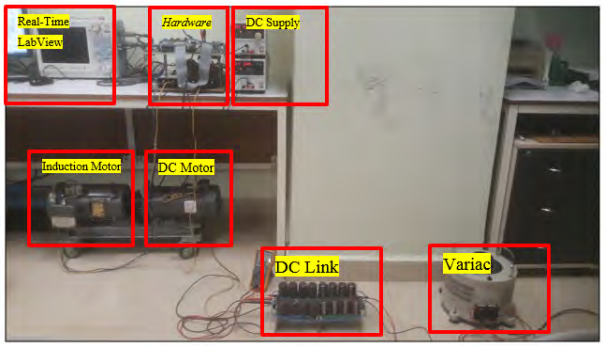

Fig. 13. Experimental setup for loaded test

The tests were conducted by varying the set point values between 500 rpm and 750 rpm as well as the load torque values. Meanwhile, the SOSMC parameter values used were the same as those applied in the no-load test.

The motor speed response obtained is shown in the following Figures 14 and 15. Figures 14 and 15 show that the speed settings of the 3-phase induction motor controlled using SOSMC were similar to those applied when no load was applied. A DC motor was added at different load torque values for the test. Moreover, it was observed that there were 5 conditions at every 20-second chance such that the first 20 seconds were without load after which load was added, and later removed. This process was repeated for different load torque values.

The results showed that the SOSMC had good dynamic performance.

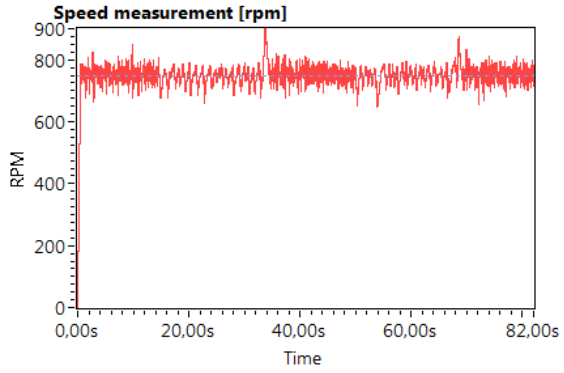

Fig. 14. SOSMC test with a set point load of 750 rpm

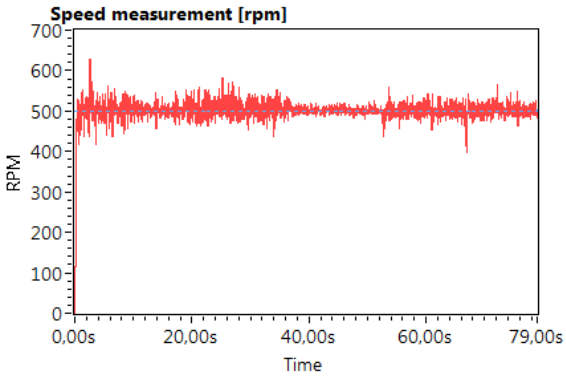

Fig. 15. SOSMC test with a set point load of 500 rpm

It was also observed from the speed response graph that the robustness was maintained at the set point value when there was a change in disturbance (load torque).

Moreover, the controller was able to maintain robustness despite the change in the load torque value from 0.8 N m to 1.3 N m. The chattering produced was found to be higher under loaded conditions compared to when there was no load. This was due to the fact that the motor had been initially burdened by the DC motor coupled with the system. It was further noted that the SOSMC controller functioned at the loading condition by bringing the motor into a sliding state, thereby, causing the control signal u to increase due to an error value. This control signal served as the electric torque (T_e) or output of the controller which was in line with I_q. The provisional of an additional load was expected to cause an increase in the I_q value.

VII. Conclusion

This study presented a scheme to reduce the chattering phenomenon in a 3-phase induction motor using the Second-Order Sliding Mode Control (SOSMC) with a super twisting algorithm at low-speed settings of IFOC.

This was required due to the difficulty in controlling the induction motor because of the excessive power losses which often lead to significant low speed response and a greater percentage of chattering in the motor. The control design procedures and system stability analysis were demonstrated and this was followed by the implementation of the scheme in real-time using Labview software. The simulation results showed that SOSMC was able to reduce the chattering phenomenon better than the FOSMC as indicated by the reduction up to 0.046 var at a set point of 100 rpm while maintaining the system robust at a steady error of 0.001%. Moreover, the experimental results showed that SOSMC reduced chattering up to 2.89 var at a set point of 100 rpm under no-load conditions, had a good dynamic performance, and guaranteed limited time convergence. It was observed that the system robustness was maintained despite the changes in the load torque values of the DC motor up to 1.3 N m. In the future, a filter can be added to get better performances.

References

[1] S. E. Farhi, D. Sakri, and N. Golea, “Sensorless Control of Induction Motor Using Second-Order Sliding Mode Algorithms,” in *Proceedings - 2019 1st International Conference on Sustainable Renewable Energy Systems and Applications, ICSRESA 2019*, 2019, pp. 6–11. doi: 10.1109/ICSRESA49121.2019.9182616

[2] A. Wahyu Aditya, M. Rizani Rusli, B. Praharsena, E. Purwanto, D. Cahya Happyanto, and B. Sumantri, The Performance of FOSMC and Boundary - SMC in Speed Controller and Current Regulator for IFOC-Based Induction Motor Drive, in *Proceedings - 2018 International Seminar on Application for Technology of Information and Communication: Creative Technology for Human Life, iSemantic 2018*, 2018, pp. 139–144. doi: 10.1109/ISEMANTIC.2018.8549842

[3] A. W. Aditya, R. M. Utomo, Hilmansyah, E. Purwanto, M. R. Rusli, and B. Praharsena, Power performance of boundary technique on FOSMC based induction motor drives, *J. Phys. Conf. Ser.*, vol. 1450, p. 012042, Feb. 2020. doi: 10.1088/1742-6596/1450/1/012042

[4] Muntashir, A., Purwanto, E., Sumantri, B., Chattering Reduction Using Boundary-SMC on Low-Speed Setting of 3-Phase Induction Motor with IFOC Method, (2022) *International Review of Automatic Control (IREACO)*, 15 (1), pp. 1-11. doi: https://doi.org/10.15866/ireaco.v15i1.21250

[5] J. R. Riba, C. López-Torres, L. Romeral, and A. Garcia, Rare-earth-free propulsion motors for electric vehicles: A technology review, *Renew. Sustain. Energy Rev.*, vol. 57, pp. 367–379, 2016. doi: 10.1016/j.rser.2015.12.121

[6] A. Parthan, L. Padma Suresh, and A. Raj, SMC and FOC: Comparative investigation of sliding mode and field oriented control of induction motor, *Int. J. Recent Technol. Eng.*, vol. 8, no. 1, pp. 316–321, 2019.

[7] E. Quintero-Manríquez, E. N. Sanchez, and R. A. Félix, Real-time direct field-oriented and second order sliding mode controllers of induction motor for electric vehicles applications, in *2015 10th System of Systems Engineering Conference, SoSE 2015*, 2015, pp. 220–225. doi: 10.1109/SYSOSE.2015.7151989

[8] A. A. Muntashir, E. Purwanto, B. Sumantri, H. H. Fakhruddin, and R. A. N. Apriyanto, Static and dynamic performance of vector control on induction motor with PID controller: An investigation on labVIEW, *Automot. Exp.*, vol. 4, no. 2, pp. 83–96, 2021. doi: 10.31603/ae.4812

[9] A. Dannier, A. Del Pizzo, L. P. Di Noia and S. Meo, Integral sliding-mode direct torque control of sensorless induction motor drives, 2017 *IEEE International Symposium on Sensorless Control for Electrical Drives (SLED)*, 2017, pp. 243-248. https://doi.org/10.1109/SLED.2017.8078457

[10] M. P. Jati et al., A fuzzy supervisory scalar control for matrix converter induction motor drives, *Int. J. Electr. Eng. Informatics*, vol. 13, no. 1, pp. 203–217, 2021. doi: 10.15676/IJEEI.2021.13.1.12

[11] J. L. Febin Daya, V. Subbiah, A. Iqbal, and S. Padmanaban, Novel wavelet-fuzzy based indirect field oriented control of induction motor drives, *J. Power Electron.*, vol. 13, no. 4, pp. 656–668, 2013. doi: 10.6113/JPE.2013.13.4.656

[12] Y. Kalil et al., Speed Control of a Five-Phase Induction Motor Drive using Modified Super-Twisting Algorithm, in *SPEEDAM 2018 - Proceedings: International Symposium on Power Electronics, Electrical Drives, Automation and Motion*, 2018, vol. 1, pp. 938–943. doi: 10.1109/SPEEDAM.2018.8445404

[13] M. Kokare and P. A. Kulkarni, Performance Analysis of Speed Control of PMDC Motor using Fuzzy Logic Controller, *Int. Res. J. Eng. Technol.*, vol. III, no. July, pp. 2958–2963, 2019.

[14] A. Ammar, A. Bourek, and A. Benakcha, Implementation of robust SVM-DTC for induction motor drive using second order sliding mode control, in *Proceedings of 2016 8th International Conference on Modelling, Identification and Control, ICMIC 2016*, 2017, pp. 338–343. doi: 10.1109/ICMIC.2016.7804133

[15] H. Benbouhenni and N. Bizon, Third-order sliding mode applied to the direct field-oriented control of the asynchronous generator for variable-speed contra-rotating wind turbine generation systems, *Energies*, vol. 14, no. 18, pp. 1–20, 2021. doi: 10.3390/en14185877

[16] L. Zhang, H. Zhang, H. Obeid, and S. Laghrouche, Time-varying state observer based twisting control of linear induction motor considering dynamic end effects with unknown load torque, *ISA Trans.*, vol. 93, pp. 290–301, 2019. doi: 10.1016/j.isatra.2019.03.008

[17] M. Z. Kari, A. Mechernene, S. M. Meliani, and I. Guenoune, Super-Twisting strategy based indirect field oriented control without using the currents sensor: Application to IM ∗, in *Proceedings of 2018 3rd International Conference on Electrical Sciences and Technologies in Maghreb, CISTEM 2018*, 2019, pp. 1–6. doi: 10.1109/CISTEM.2018.8613540

[18] Bimal K. Bose, *Power Electronics and Motor Drives: Advances and Trends, Second Edition*. Elsevier Inc., 2020.
[19] Z. Mekrini and S. Bri, Performance of an indirect field-oriented control for asynchronous machine, *Int. J. Eng. Technol.*, vol. 8, no. 2, pp. 726–733, 2016.
[20] N. Zaidi, M. Jemli, H. Ben Azza, and M. Boussak, A time-varying gain super-twisting algorithm to drive a SPIM, *J. Power Electron.*, vol. 13, no. 6, pp. 955–963, 2013.
doi: 10.6113/JPE.2013.13.6.955
[21] J. Listwan and K. Pieńkowski, Control of five-phase induction motor with application of second-order sliding-mode Direct Field-Oriented method, *2017 International Symposium on Electrical Machines (SME)*, Naleczow, Poland, 2017, pp. 1-6.
doi: 10.1109/ISEM.2017.7993553
[22] B. Sumantri, N. Uchiyama, and S. Sano, Generalized super-twisting sliding mode control with a nonlinear sliding surface for robust and energy-efficient controller of a quad-rotor helicopter, in *Proceedings of the Institution of Mechanical Engineers, Part C: Journal of Mechanical Engineering Science*, 2017, vol. 231, no. 11, pp. 2042–2053.
doi: 10.1177/0954406216628897
[23] Shaija, P., Daniel, A., Parameter Tuning of Sliding Mode Speed Controller of Induction Motor Drive Using Teaching-Learning Based Optimization Algorithm, (2022) *International Review of Automatic Control (IREACO)*, 15 (1), pp. 28-37.
doi: https://doi.org/10.15866/ireaco.v15i1.21953
[24] Makhad, M., Zazi, K., Zazi, M., Loulijat, A., Smooth Super Twisting Sliding Mode Control for Permanent Magnet Synchronous Generator Based Wind Energy Conversion System, (2020) *International Journal on Energy Conversion (IRECON)*, 8 (5), pp. 171-180.
doi: https://doi.org/10.15866/irecon.v8i5.19362
[25] Dbaghi, Y., Farhat, S., Mediouni, M., Essakhi, H., Comparative Study Between Back-Stepping Control and ANN-Sliding Mode Control of DFIG-Based Wind Turbine System, (2021) *International Review on Modelling and Simulations (IREMOS)*, 14 (4), pp. 261-271.
doi: https://doi.org/10.15866/iremos.v14i4.19376
[26] Traoré, B., Doumiati, M., Olivier, J., Morel, C., Adaptive Power Sharing Algorithm Combined with Robust Control for a Multi-Source Electric Vehicle: Experimental Validation, (2022) *International Review of Electrical Engineering (IREE)*, 17 (1), pp. 39-53.
doi:https://doi.org/10.15866/iree.v17i1.21269
[27] Tran, C., Brandstetter, P., Kuchar, M., Ho, S., A Novel Speed and Current Sensor Fault-Tolerant Control Based on Estimated Stator Currents in Induction Motor Drives, (2020) *International Review of Electrical Engineering (IREE)*, 15 (5), pp. 344-351.
doi:https://doi.org/10.15866/iree.v15i5.17937
[28] Hassan, M., Humaidi, A., Hamza, M., On the Design of Backstepping Controller for Acrobot System Based on Adaptive Observer, (2020) *International Review of Electrical Engineering (IREE)*, 15 (4), pp. 328-335.
doi:https://doi.org/10.15866/iree.v15i4.17827

Authors' information

[1]Department of Electrical Engineering, Politeknik Elektronika Negeri Surabaya, Surabaya, Indonesia.

[2]Department of Mechatronics Engineering, Politeknik Astra, Jakarta, Indonesia.

Era Purwanto (Corresponding Author) is a lecturer of Politeknik Elektronika Negeri Surabaya (PENS), Indonesia. He received a bachelor's degree in Electrical Engineering from Institut Teknologi Sepuluh Nopember (ITS), Indonesia, M.Eng (Master of Engineering) from Shizuoka University, Japan, and Doctor of Engineering from ITS, Indonesia. His research interest is the electrical machine, intelligent control, electric drive, and power electronics.
E-mail: era@pens.ac.id

Abdillah Aziz Muntashir is a lecturer of Astra Polytechnic, Jakarta, Indonesia. He received bachelor and master degree in Electrical Engineering from Politeknik Elektronika Negeri Surabaya (PENS), Surabaya, Indonesia. His research interest is in power electronics, electric machines, electrical drive, and control systems.

Muhammad Rizani Rusli is a lecturer in department of electrical engineering, Politeknik Elektronika Negeri Surabaya (PENS), Surabaya, Indonesia. He received his bachelor and master degree in electrical engineering from PENS in 2017 and 2019. He had experience as a research engineer in Center of Excellence - System and Control of Automotive, Institut Teknologi Sepuluh Nopember, Surabaya, Indonesia (2017-2020). He is also had experience as research and development engineer of PT. Garda Energi Nasional Indonesia, Sidoarjo, Indonesia (2020-2022). His research interests are related to power electronics, electric drives, electric machines, and control system.

Bambang Sumantri is a lecturer of Politeknik Elektronika Negeri Surabaya (PENS), Indonesia. He received a bachelor's degree in Electrical Engineering from Institut Teknologi Sepuluh Nopember (ITS), Indonesia, M.Sc (Master of Science) in Control Engineering from Universiti Teknologi Petronas, Malaysia, and Doctor of Engineering in Mechanical Engineering, Toyohashi University of Technology, Japan. His research interest is in the robust control system, robotics, and embedded control system.